Research Article

Yong Wang, Chengyi Zhu, Guangqiang Li*, Yu Liu, and Bowen Zhou

The effect of Nb content on precipitates, microstructure and texture of grain oriented silicon steel

https://doi.org/10.1515/htmp-2019-0010
Received Nov 01, 2018; accepted Jan 02, 2019

Abstract: Niobium has the potential as an inhibitor forming element in grain oriented silicon steel. The grain oriented silicon steels with different Nb contents (0.028 wt% and 0.052 wt%) were prepared, and the effect of Nb content on the evolution of precipitates, microstructure and texture were investigated by the various analysis methods and thermodynamic calculations. The results show that the smaller size and larger number density of precipitates were obtained in the sample with low Nb steel after hot rolling. In the process of normalization, Nb(C, N) are more inclined to precipitate along the dislocations caused by hot rolling, contributing to finer and more dispersed precipitates in normalized bands. The finer and more dispersed precipitates in 0.028% Nb containing silicon steel perform a stronger pinning force during whole heat treatment processes, resulting in the smaller grain size and higher intensity of Goss texture in the specimen containing 0.028% Nb. After normalization, the intensities of Goss texture in both steels decrease.

Keywords: Grain oriented silicon steel; niobium; precipitates; texture

***Corresponding Author: Guangqiang Li:** State Key Laboratory of Refractories and Metallurgy; Wuhan University of Science and Technology, Wuhan 430081, China; Key Laboratory for Ferrous Metallurgy and Resources Utilization of Ministry of Education; Wuhan University of Science and Technology, Wuhan 430081, China; Collaborative Innovation Center of Steel Technology, University of Science and Technology Beijing, Beijing, 100083, China; Email: liguangqiang@wust.edu.cn; Tel.: +86 27 68862665; Fax: +86 27 68862665

Yong Wang, Chengyi Zhu, Yu Liu: State Key Laboratory of Refractories and Metallurgy; Wuhan University of Science and Technology, Wuhan 430081, China; Key Laboratory for Ferrous Metallurgy and Resources Utilization of Ministry of Education; Wuhan University of Science and Technology, Wuhan 430081, China

Bowen Zhou: Technical center of Liuzhou Iron and Steel Group Co., Ltd., Liuzhou, Guangxi 545000, China

1 Introduction

Grain oriented silicon steel is an important soft magnetic material in electricity and electronic devices, which is widely used as the materials for different transformers owing to its high magnetic permeability and low core loss [1]. And it's the only product manufactured in the steel industry that applies the secondary recrystallization phenomenon. The manufacturing process of grain oriented silicon steel includes basic oxygen furnace (BOF) steelmaking, secondary refining and continuous casting, slab reheating, hot rolling, normalizing annealing, cold rolling, decarburization annealing, secondary recrystallization annealing, heat flattening coating, and so on. The excellent magnetic properties are related to the sharpness of Goss texture ({110} <001>), the investigations on Goss texture have been widely carried out during several decades [1–4]. In order to obtain the sharp Goss texture, the fine and dispersed precipitates called inhibitors play an important role during the manufacturing process of grain oriented silicon steel. Generally, there are two ways to obtain the inhibitors for grain oriented silicon steel, namely, the inherent inhibitor method [5] and the acquired inhibitor method [6]. The inherent inhibitors are mainly MnS, which are acquired by adding inhibitor elements during steelmaking, and precipitating during hot rolling or normalization [7]. And the acquired inhibitors are acquired by nitriding after decarburization annealing [8]. However, two methods would consume a large amount of energy and increase the production cost of grain oriented silicon steel because the higher reheating temperature and the complicated nitriding process. Thus, Nb(C, N) [9, 10] and Cu_2S [11, 12] are considered to be used as inhibitors in grain oriented silicon steel, which have lower solution temperature so that the slab reheating temperature can be decreased.

Previous studies confirmed that Nb(C, N) as inhibitor for grain oriented silicon steel is feasible. N.H. van Dijk *et al.* [13] found that the particles with the size smaller than 10 nm mainly correspond to Nb(C, N) precipitates and the

Table 1: Chemical compositions of tested silicon steel (wt%)

Sample	C	Si	Mn	S	Als	Nb	N	Fe
S1	0.057	3.28	0.04	0.0009	0.0042	0.028	0.008	Balance
S2	0.053	3.31	0.04	0.0008	0.0047	0.052	0.008	Balance

larger particles to MnS precipitates in high-strength low-alloy steel. It indicates that the size of Nb(C, N) precipitates is suitable to be used as inhibitor in grain oriented silicon steel, while the characteristics of Nb(C, N) precipitates were not well studied. Klaus Hulka *et al.* [9] investigated the effect of NbC as an inhibitor in niobium microalloyed 3% silicon steel, and found that the highest volume fraction of Goss texture exist below the surface in the hot rolled strip of this steel, meanwhile the core losses are the lowest in the sheet with NbC as main inhibitor, which shows that Nb(C, N) could be a suitable inhibitor. Feng *et al.* [14] confirmed that the precipitation temperature of Nb(C, N) increases significantly with the increase of Nb content in silicon steel, which does not affect the precipitation of MnS, and proper Nb addition in grain oriented silicon steel can reduce the slab reheating temperature.

However, limited researches about the influence of Nb content on the evolution of microstructure, texture and inhibitor of grain oriented silicon steel during normalization were carried out, which needs to be studied in detail.

In this study, grain oriented silicon steel containing two different Nb content were prepared. And the microstructure, texture and inhibitor of two bands before and after hot band annealing were investigated, which will provide reference data for the practical production of Nb-bearing grain oriented silicon steel.

2 Materials and Experimental Procedure

Grain oriented silicon steels containing different Nb contents were melted by a 100 kg vacuum induction furnace around 1530°C and were cast into 210 mm × 120 mm × (30–50) mm square ingot. The main chemical composition of the specimens is listed in Table 1. Both ingots were reheated at 1250°C for 2.5 hours, and then were hot rolled to 2.6 mm in thickness, the start and finish rolling temperature was 1000°C and 940°C, respectively. Subsequently, both hot-rolled bands were normalized at 920°C for 3 minutes.

The precipitates along the transverse section (RD–TD) of hot-rolled bands and normalized bands were extracted by carbon extraction replica technique and analyzed by JEM-2100 transmission electron microscopy (TEM), one hundred TEM images at ×20 000 magnifications were taken for each specimen, the number density and size of the precipitates were measured by using an Image-Pro Plus image analysis software. The composition and morphology of the precipitates were characterized by TEM equipped with energy dispersive X-ray spectroscopy (EDS).

The microstructure and texture of hot-rolled bands and normalized bands were determined by electron backscattered diffraction (EBSD) system equipped at Quanta 450 FEG field emission scanning electron microscope (FE-SEM). The EBSD measurements were carried out along the longitudinal section (RD–ND) of specimens. The EBSD data was analyzed by an HKL Channel 5 EBSD software.

3 Results

3.1 Particles characteristics

Mainly four kinds of inhibitors were observed in hot-rolled bands and normalized bands which are shown in Figure 1. Precipitates in Figure 1a to d were detected to be MnS (Figure 1a), complex particles of MnS and NbN (Figure 1b), complex particles of MnS, NbN and AlN (Figure 1c), and NbC (Figure 1d), respectively. It should be noticed that the carbon replica specimens for precipitates observation were examined by TEM. The distribution of carbon in EDS elemental mapping analysis is affected by carbon replica specimen. As a result, there are no obvious differences in the distribution of carbon in Figure 1d. In order to further investigate the impact of Nb content on inhibitors, the distribution and size of precipitates on replica were observed by TEM, as shown in Figure 2, and the statistical results were shown in Figure 3. It can be seen that the average size of precipitates in hot-rolled band increases from 40 nm to 66 nm with the increase of Nb content, meanwhile the number density of precipitates in hot-rolled band decreases from $1.38\times10^6/mm^2$ to $9.4\times10^5/mm^2$, as shown in Figure 3a. After normalization, Figure 2c and 2d exhibits more disperse distribution of second phase particles

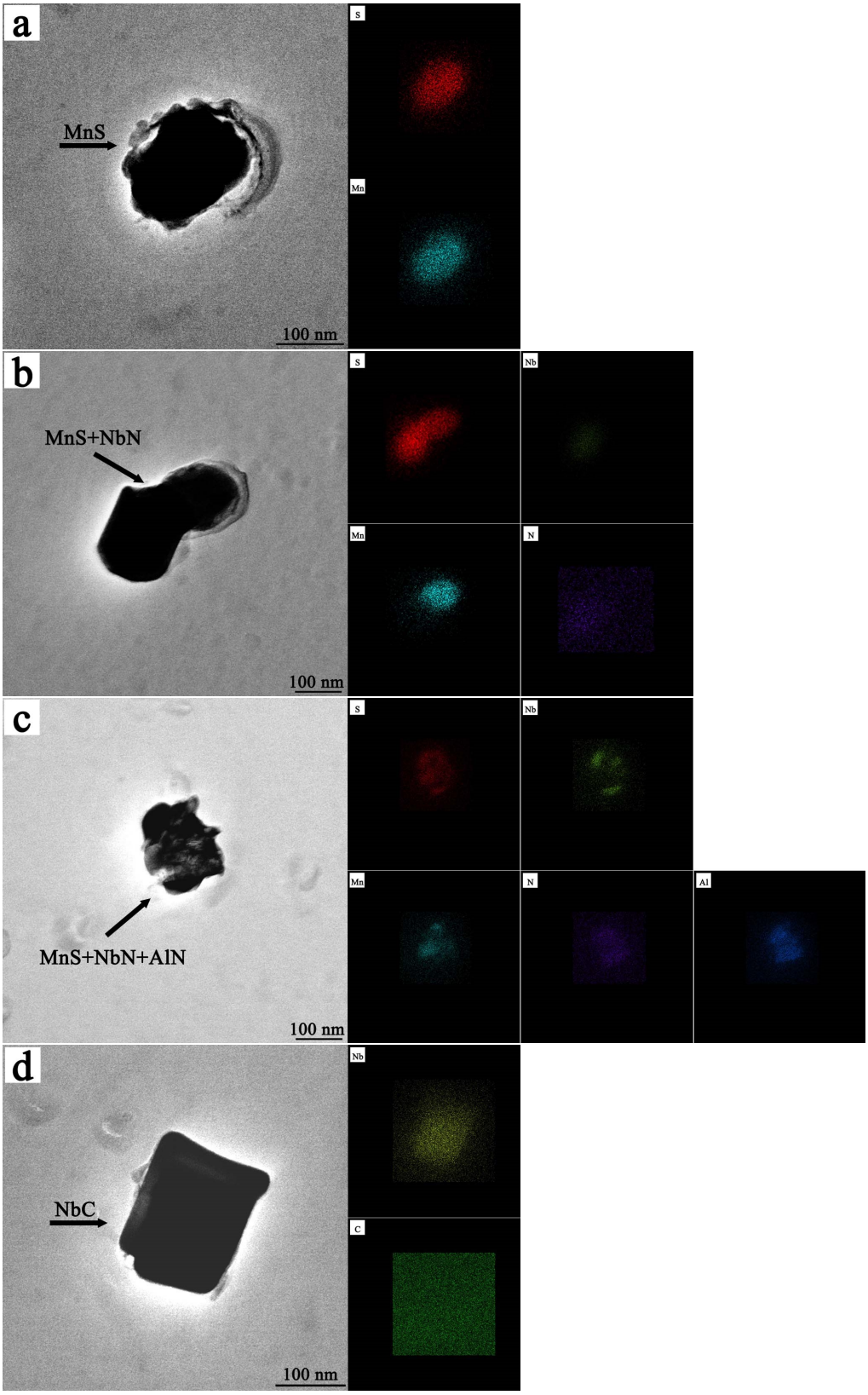

Figure 1: Precipitates morphologies observed by TEM and EDS elemental mapping of precipitates: (a)MnS, (b)MnS+NbN, (c)MnS+NbN+AlN, and (d)NbC

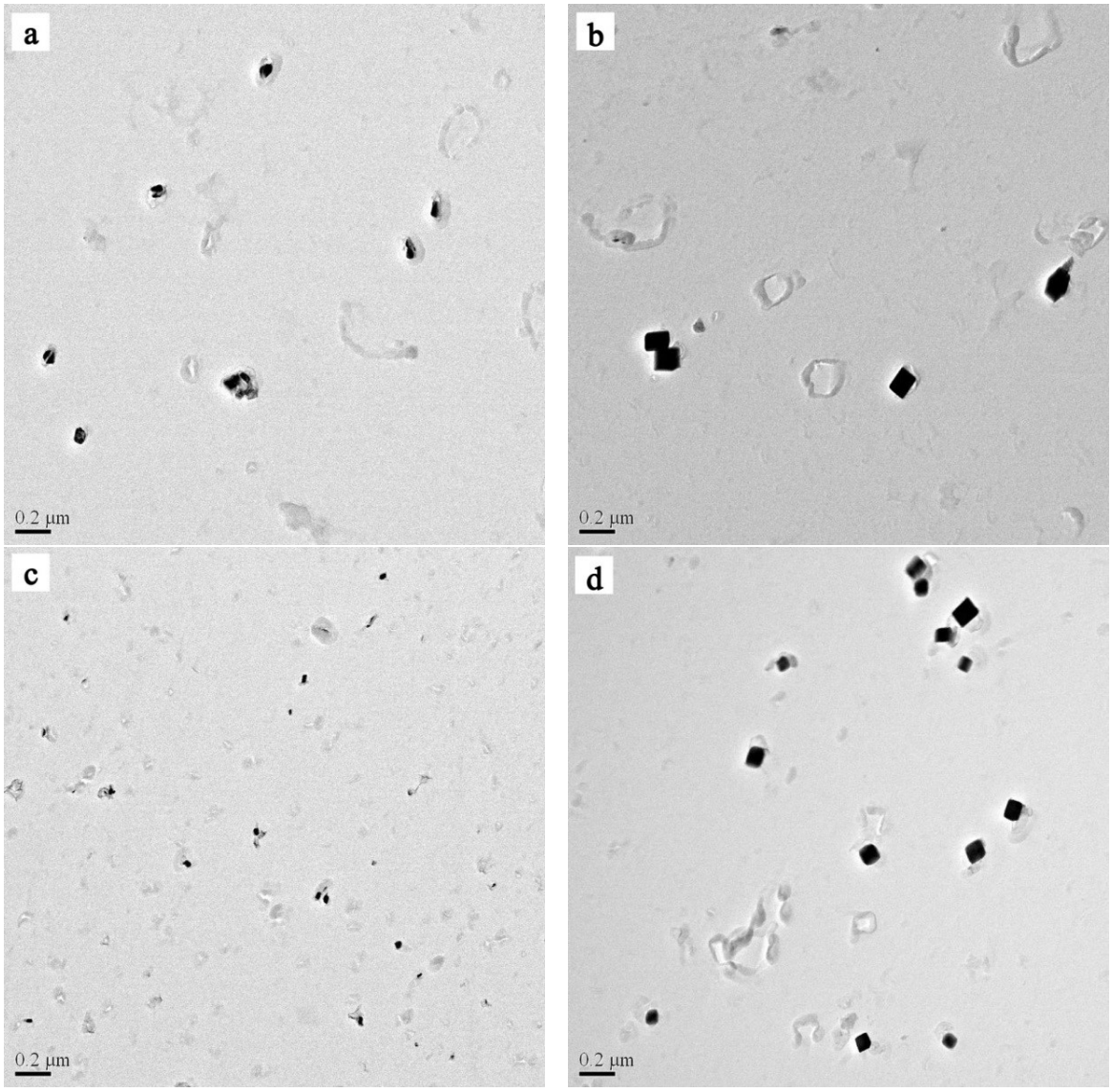

Figure 2: TEM images of precipitates in (a) S1-hot rolled, (b) S2-hot rolled, (c) S1-normalized, and (d) S2-normalized

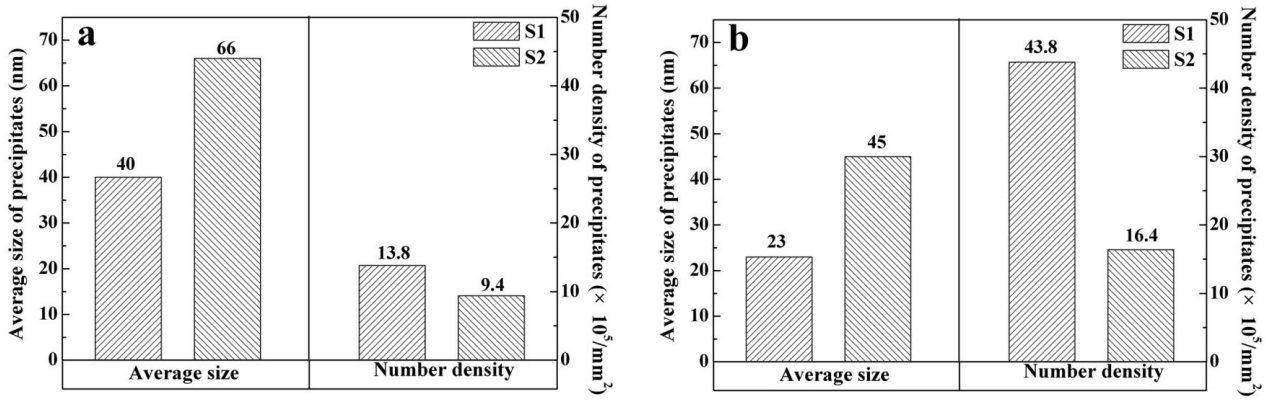

Figure 3: Size and number density of precipitates in (a) hot-rolled sheet, (b) normalized sheet

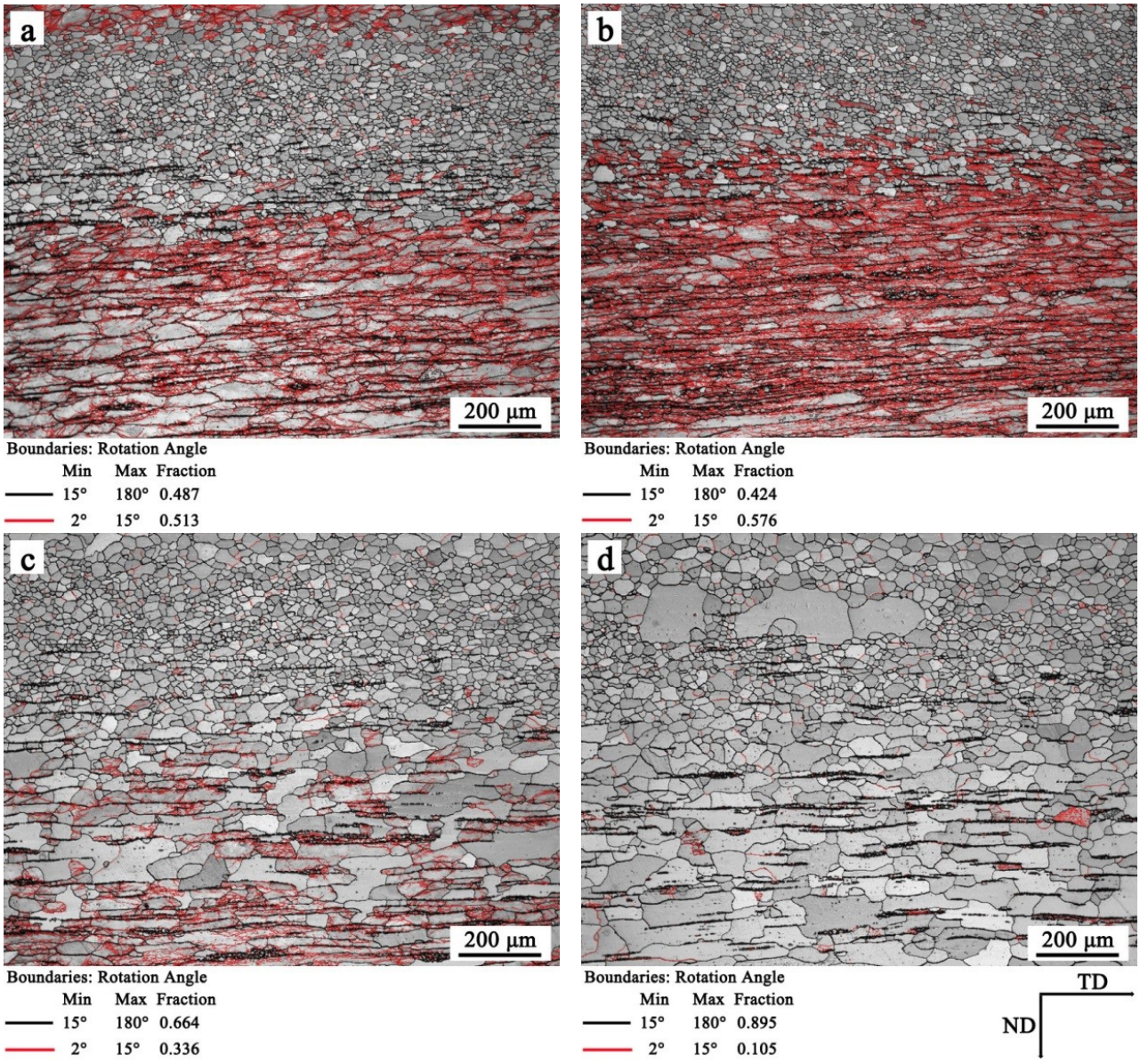

Figure 4: Microstructure of (a) S1-hot rolled, (b) S2-hot rolled, (c) S1-normalized, and (d) S2-normalized

and the average size of precipitates decreases obviously compared to hot-rolled bands. Compared the two normalized bands, the average size of precipitates in normalized band increases from 23 nm to 45 nm with the increase of Nb content, meanwhile the number density of precipitates in normalized band decreases from $4.38\times10^{6}/mm^{2}$ to $1.64\times10^{6}/mm^{2}$, as shown in Figure 3b.

3.2 Microstructure and texture of hot-rolled band and normalized band

The microstructure and texture of hot-rolled band and normalized band were observed through EBSD. Figure 4 shows the microstructure of hot-rolled band and normalized band, each figure is a 1/2 cross section of the sample perpendicular with transverse direction (TD). It can be seen that the microstructure along the thickness is inhomogeneous due to the different amounts of deformation and the temperature gradient along the thickness. The surface region consists of fine equiaxed grains, the elongated grains and deformed structures exist in subsurface region

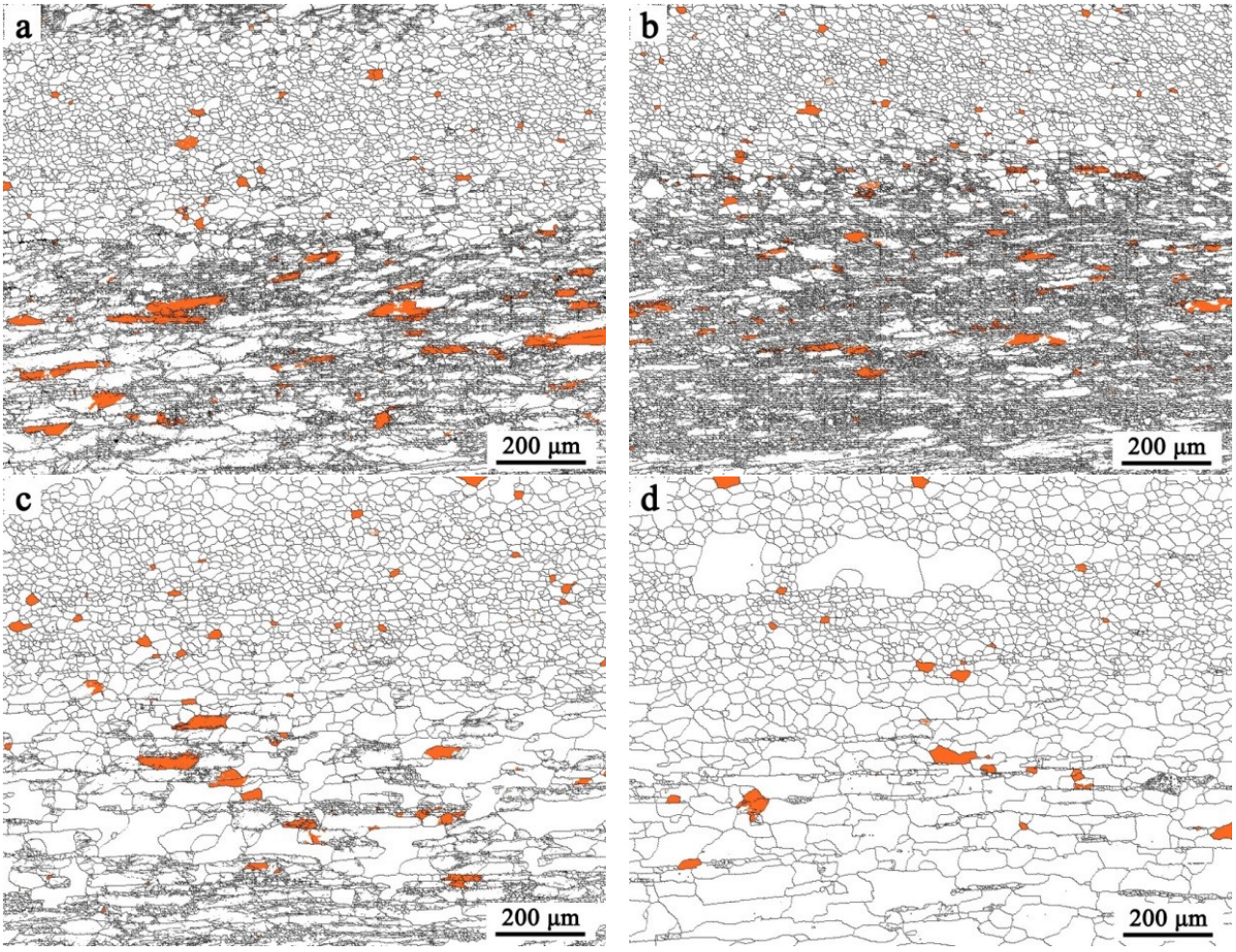

Figure 5: Goss texture of (a) S1-hot rolled, (b) S2-hot rolled, (c) S1-normalized, and (d) S2-normalized (Orange zone is Goss texture within 10° of exact Goss orientation)

and the center region, the average grain diameter of S1-hot rolled and S2-hot rolled is 14.56 μm and 12.64 μm, respectively, as shown in Figure 4a and b. After normalization, Figure 4c and d show that the normalized bands had experienced an obvious recrystallization process. The surface region shows coarse equiaxed grains, and the microstructure in subsurface region and center region of normalized bands recrystallized and grow up along the rolling direction. The average grain diameter of S1-normalized and S2-normalized is 17.89 μm, and 20.77 μm, respectively.

The distribution map of Goss component was shown in Figure 5. From Figure 5a and b, it can be seen that the Goss texture mainly located at subsurface region, and most of them are deformed structures. The volume fraction of Goss texture in S1-hot rolled and S2-hot rolled is 3.4% and 2.3%, respectively. After normalization, the Goss texture existed in subsurface of hot-rolled band which have been proved as the origin of sharp Goss texture component in fully processed silicon steels [2, 15] still exists in the subsurface of normalized band but the volume fraction of Goss texture in S1-normalized and S2-normalized decreased to 1.9% and 1.1%, respectively.

The ideal preferred orientations of cubic structure materials in the Euler space are located at the orientation distribution function (ODF) maps at $\varphi_2 = 45°$, as shown in Figure 6. To further investigate the impact of Nb content on the texture of grain oriented silicon steel, the graph of $\varphi_2 = 45°$ sections of the orientation distribution functions (ODF) of hot-rolled band and normalized band was shown in Figure 7. According to Figure 7a and b, it can be seen that the main components of texture in S1-hot rolled and S2-hot rolled specimens are {112} <111> and {110} <001>, and {001} <110> texture was observed in S2-hot rolled. The intensity of Goss texture component in S1-hot rolled and S2-hot rolled is around 6.1 and 4.2, respectively. After normalization, the Goss texture exists in S1-normalized and

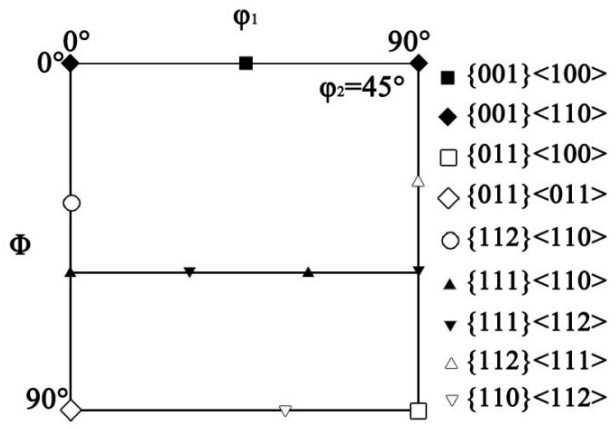

Figure 6: Ideal preferred orientations in the Euler space

S2-normalized is still the main texture component, meanwhile, the intensity of {001} <100> texture, {001} <110> texture and {112} <111> texture decrease to a certain extent. The intensity of Goss texture component in S1-normalized and S2-normalized decreased to around 3.6 and 2.4, respectively, as shown in Figure 7c and d.

4 Discussion

4.1 Effect of Nb content on precipitates

The thermodynamic calculation results calculated by JMatPro were shown in Figure 8 and Figure 9. Figure 8 shows the curves of different inhibitors content varying with the temperature. In both silicon steels with different Nb contents, Nb(C, N), and AlN were sequentially precipitated with the temperature decreases. And the main precipitate in two samples is Nb(C, N). With the increase of Nb content, the precipitation start temperature of AlN changed little, which is different to Feng *et al.*'s [14] results, it may be attributed to the little Al_s content in the present study. But the precipitation start temperature of Nb(C, N) increases from 1220°C to 1280°C, which means that the precipitation start temperature of Nb(C, N) in S2 is higher than that in S1. And both the precipitation finish temperature of Nb(C, N) in two samples are 920°C. Figure 9 shows the proportion changes of liquid, ferrite and austenite with temperature. During the cooling process, the liquid disappears firstly, and then ferrite starts to precipitate, the percentage of ferrite decreases firstly and then increase, when the temperature cools down to 1150°C, the percentage of ferrite reaches to the minimum. The change of austenite content is in con-

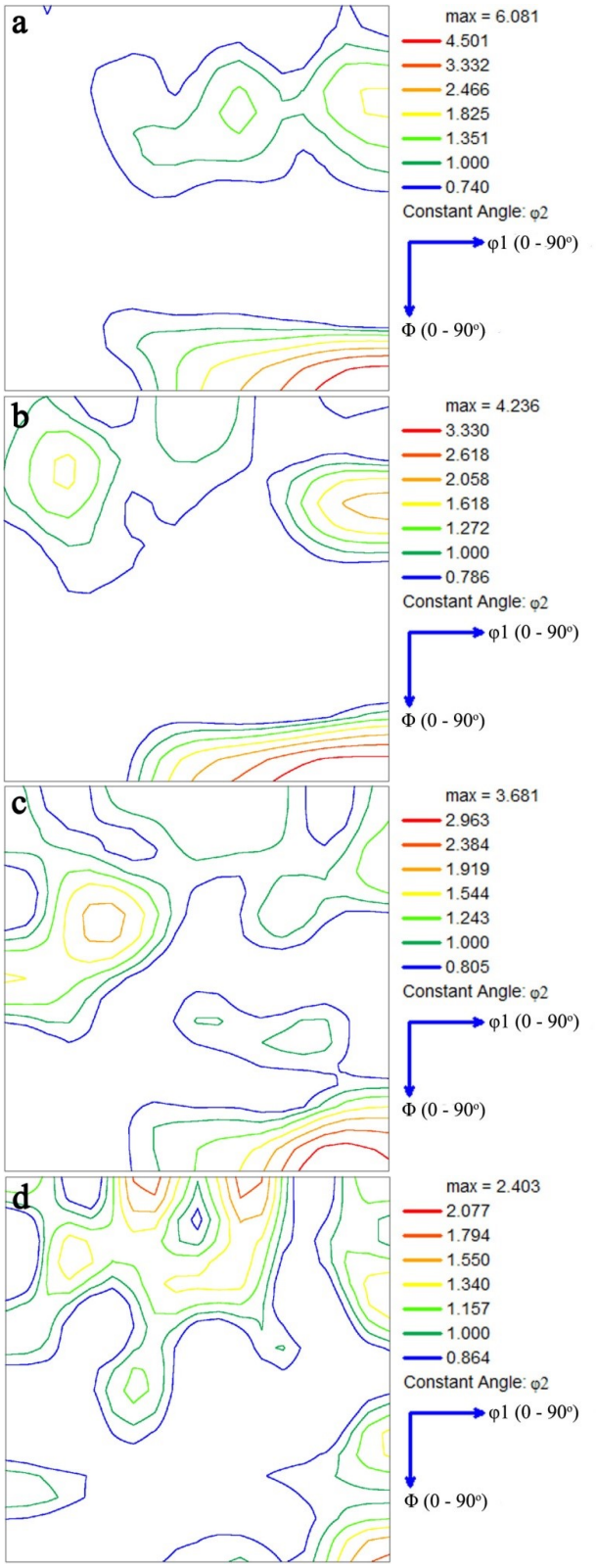

Figure 7: ODFs at $\varphi_2 = 45°$ of (a) S1-hot rolled, (b) S2-hot rolled, (c) S1-normalized, and (d) S2-normalized

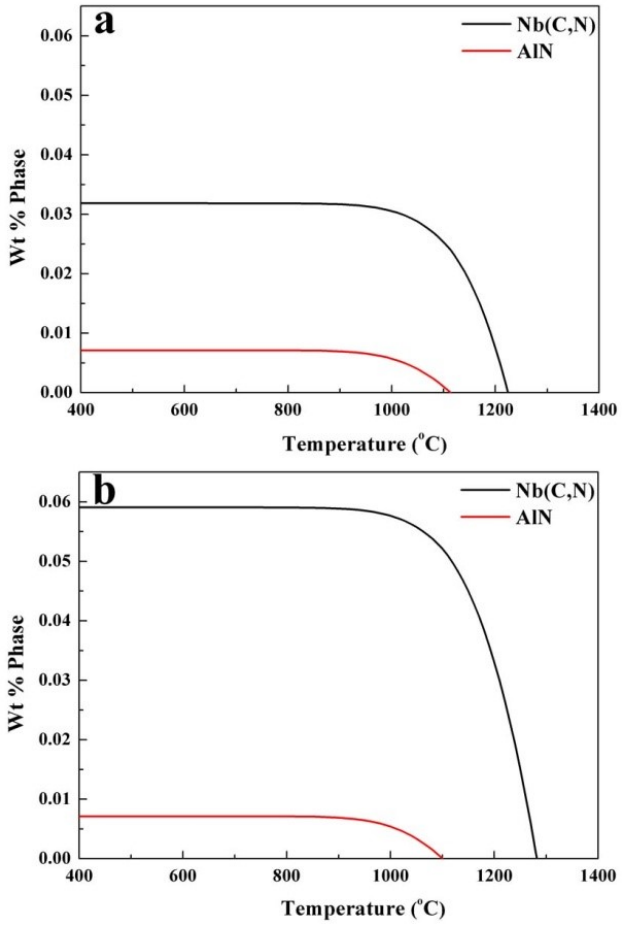

Figure 8: Precipitates content varies with the temperature (a) 0.028% Nb, (b) 0.052% Nb

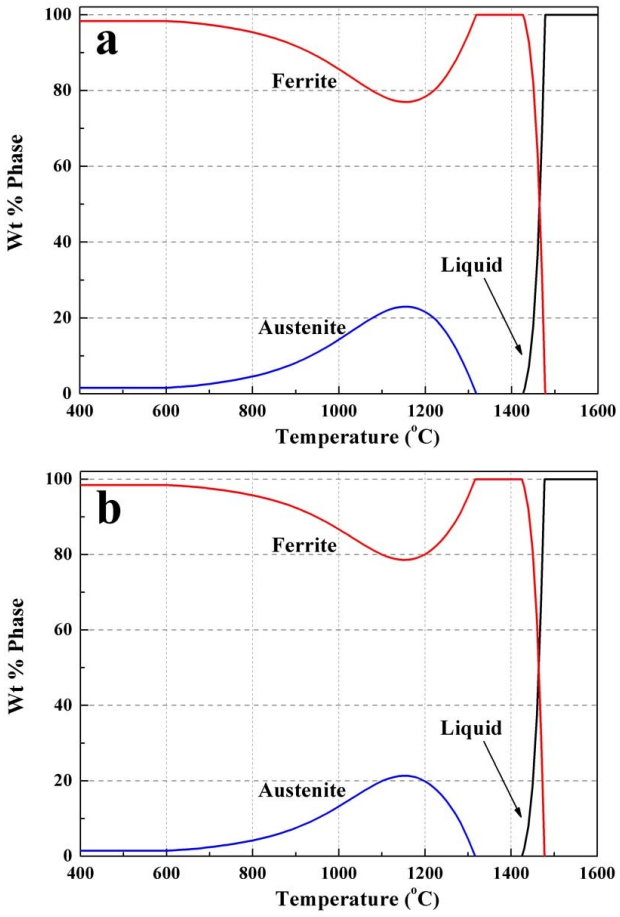

Figure 9: Phase diagram of silicon steels with different Nb contents (a) 0.028% Nb, (b) 0.052% Nb

trast to that of ferrite content. It should be noticed that the maximum value of austenite content decreases with the increase of Nb content. Previous researches show that the solubility of Nb(C, N) in austenite is different from that in ferrite, and the solubility product of Nb(C, N) in austenite and ferrite can be estimated by following equations [16], where T is temperature in Kelvin, [Nb], [C], and [N] represent mass percentage of the elements, subscript γ and α represent austenite and ferrite respectively:

$$\log [Nb]_{\gamma}[C]_{\gamma} = -\frac{7407}{T} + 2.783, \quad (1)$$

$$\log [Nb]_{\gamma}[N]_{\gamma} = -\frac{9940}{T} + 3.82, \quad (2)$$

$$\log [Nb]_{\alpha}[C]_{\alpha} = -\frac{11030}{T} + 4.90, \quad (3)$$

$$\log [Nb]_{\alpha}[N]_{\alpha} = -\frac{12000}{T} + 4.93. \quad (4)$$

Table 2: Dissolution temperature of inhibitors /°C

Inhibitors	Sample 1		Sample 2	
	NbC	NbN	NbC	NbN
Austenite	1054	1058	1113	1107
Ferrite	1160	1125	1205	1170

According to the equations, dissolution temperature of NbC and NbN in two samples is shown in Table 2. It can be seen that the dissolution temperature of NbC and NbN in austenite is lower than that in ferrite. Before hot rolling, the ingots were reheated to 1250°C for 2.5 hours, from Figure 8, the Nb(C, N) in S1 could completely dissolved into matrix, but the Nb(C, N) in S2 could only partly dissolved into matrix. During hot rolling process, the C, N and Nb atoms start to form Nb(C, N) as the temperature decreasing. Comparing to S1, the precipitation start temperature of NbC and NbN of S2 is higher, and the diffusion of atoms become faster at higher temperature, thus there is much more time for Nb(C, N) in S2 to generate and grow up. As

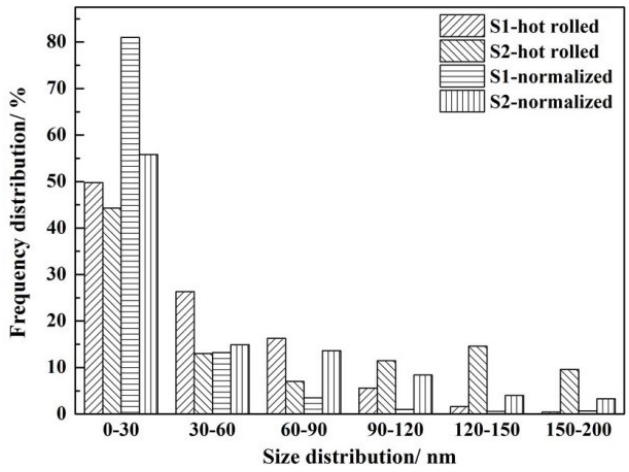

Figure 10: Size distribution of precipitates

a result, finer and more dispersed precipitates were obtained in S1, as shown in Figure 2a, b and Figure 3a. The former researches [17, 18] show that Nb(C, N) precipitate more randomly due to additional nucleation sites such as dislocations and sub-boundaries caused by hot deformation. Therefore, a great deal of supersaturated C, N and Nb atoms caused by rapid cooling rate during hot rolling completely precipitate during normalization, resulting in smaller size and larger number density of precipitates in normalized bands, as shown in Figure 2c and d. From Figure 10, it can be seen that the frequency of precipitates smaller than 30 nm after normalization increases significantly, especially for S1. Comparing to S2, the precipitation start temperature of Nb(C, N) in S1 is lower, the precipitation time is shorter during hot rolling. Hence, the supersaturated C, N and Nb atoms in S1 is much more than that in S2, which causes a larger increase in number density of precipitates compared to S2 after normalization, as shown in Figure 3b.

4.2 Effect of Nb content on microstructure and texture

It's well known that the shear deformation caused by the friction between the roller and strip surface decreased gradually from surface layer to center layer during hot rolling process, which leads to a higher dislocation density and higher stored energy in surface layer, and hence recrystallization occurs, resulting in fine exquiaxed grains in surface layer. Whereas, the microstructure in subsurface layer and center layer is elongated grains and deformed structures due to the lower stored energy. Therefore, a large number of small angle grain boundaries are obtained in hot-rolled band, as shown in Figure 4a and b. Generally, recovery consists of the cancellation and rearrangement of dislocations, which lead to form subgrains, and recrystallization is characterized by the nucleation and movement of large angle grain boundaries [19]. Figure 11 shows the misorientation angle distribution of S1 and S2 before and after normalization, which can be used to characterize recovery and recrystallization. It can be seen that a large number of small angle boundaries exist in hot-rolled bands, after normalization, the intensity of small angle boundaries decreases, while the intensity of large angle boundaries increases in normalized bands, which means the recovery and recrystallization occur during normalization. Meanwhile, the small grains in surface of hot-rolled can grow up continuously during normalization [4]. Hence, the average grain size of normalized bands increases comparing to that of hot-rolled bands, as shown in Figure 4. After normalization, it should be noticed that the average grain size of S1 increased from 14.56 μm to 17.89 μm, while that of S2 increased from 12.64 μm to 20.77 μm. It can be explained by the stronger pinning force obtained during normalization of S1 comparing to S2. The inhibitors could hinder the movement of grain boundaries when a grain boundary is moving through a matrix with second phase particles [20], and the pinning ability can be calculated bu equation (5) [21]:

$$P_z = \frac{3f_v \cdot \gamma}{d} \tag{5}$$

Where P_z is the pining force of the inhibitors, f_v is the volume fraction of the inhibitors, γ is the grain boundary energy, and d is the average diameter of the inhibitors. Assuming that γ is a constant value, it can be concluded that the pinning force of precipitates increases as the volume fraction of precipitates increases or the average precipitate radius reduces. According to the Section 4.1, finer and more dispersed precipitates were obtained in S1-normalized, hence, the stronger pining force in S1 inhibit the grain growth during normalization, which caused the average grain size of S1-normalized is smaller than that of S2-normalized.

The origin and development of Goss texture is very important for grain oriented silicon steel. It's well known that the Goss texture is formed not by recrystallization during and after hot rolling but by slip rotation in surface layer and subsurface layer due to constrained deformation [22, 23]. So in the present study, the Goss grains mainly located in surface layer and subsurface layer, as shown in Figure 5a and b. And former researches [22] proved that stronger {110} <001> orientation can be obtained in hot rolled bands with less fraction of recrystallization. Wu *et*

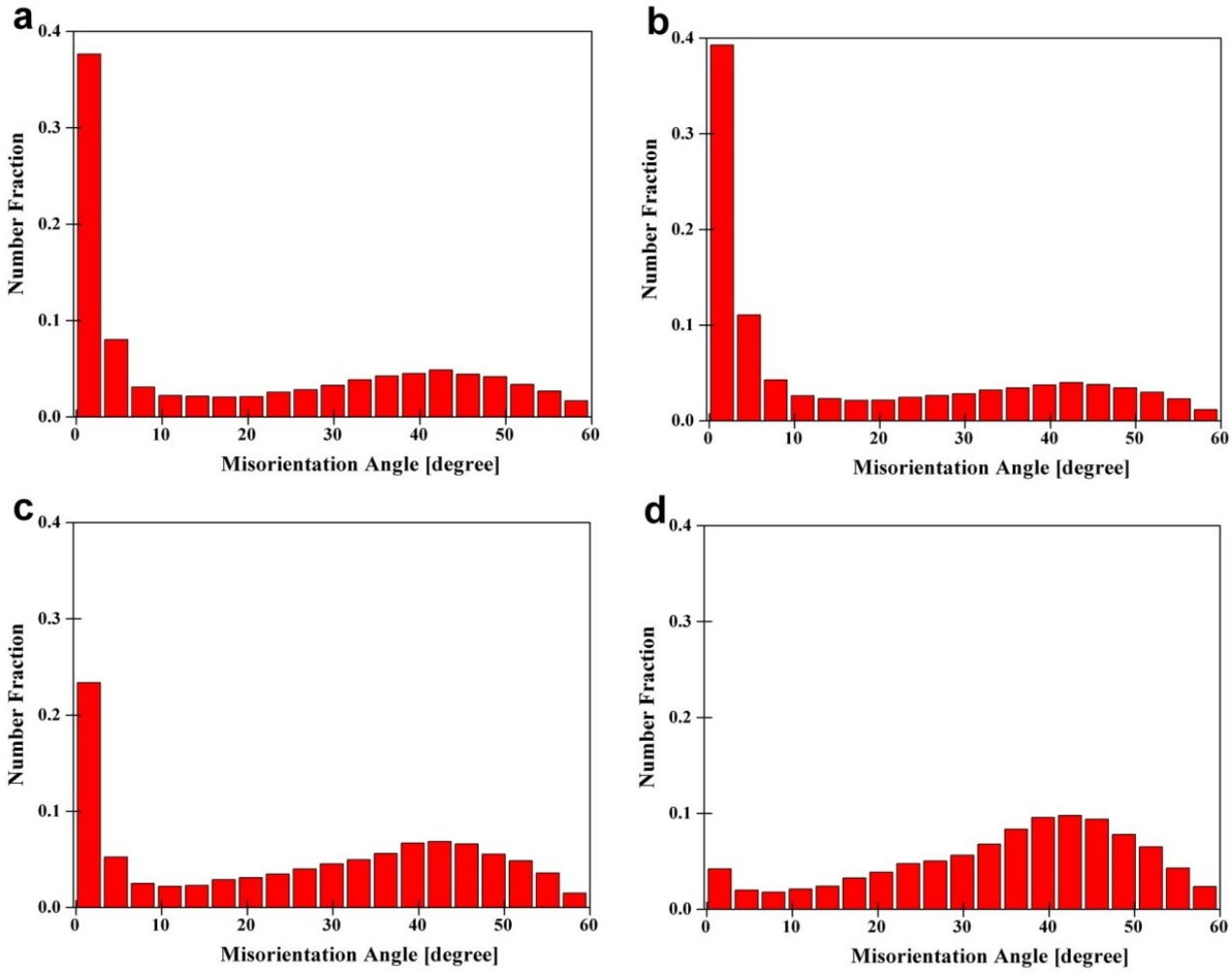

Figure 11: Misorientation angle distribution for (a) S1-hot rolled, (b) S2-hot rolled, (c) S1-normalized, and (d) S2-normalized

al. [24] reported that dynamic precipitation could retard the progress of dynamic recrystallization when the pining force is greater than driving force, which means the precipitates have an important influence on the formation of Goss texture by affecting the dynamic recrystallization during hot rolling. Hence, the value of volume fraction of Goss texture in S1-hot rolled is larger than that of in S2-hot rolled due to the smaller size and larger number density of precipitates in S1-hot rolled. After normalization, the major texture components of the hot rolled bands still exist in the normalized bands, but the intensity of the major texture components reduced, as shown in Figure 7, this result coincides with the observation results by S. M. Shin [25]. Generally, the limited phase transformation from austenite to ferrite would occur during normalization, resulting in the weakness of Goss texture after normalization [26]. Therefore, the sharpness of Goss texture in normalized bands decreases compared to hot rolled bands.

5 Conclusions

The effect of Nb content on the evolution of precipitates, microstructure and texture of grain oriented silicon steel was studied, and the results were summarized as follows:

1) The precipitates in Nb-bearing grain oriented silicon steel were MnS, compolex particles of MnS and NbN, compolex particles of MnS, NbN and AlN, and NbC.
2) During the whole heat treatment, the precipitates in the sample with 0.028% Nb show a smaller size and larger number density comparing to the sample with 0.052% Nb. After normalization, finer and more dispersed precipitates were obtained in normalized bands with 0.028% Nb.
3) The stronger pining force was obtained in normalized bands with 0.028% Nb, which inhibit the grain growth during normalization. Hence, the average grain size in normalized bands with 0.028% Nb con-

tent is smaller than that in normalized bands with 0.052% Nb.

4) The intensity of Goss texture in hot rolled bands with 0.028% Nb is 6.1, which is larger than that in hot rolled bands with 0.052% Nb due to the stronger pining force in sample with 0.028% Nb. After normalization, the intensity of Goss texture decreases.

Acknowledgement: This work was supported by the National Natural Science Foundation of China (No. 51674180) and China Postdoctoral Science Foundation (No. 2013M540609). The authors of this paper thank the National Natural Science Foundation of China and China Postdoctoral Science Foundation.

References

[1] Z. Xia, Y. Kang, and Q. Wang, J. Magn. Magn. Mater., 320 (2008) 3229-3233.
[2] Y. Inokuti, C. Maeda, Y. Ito, and H. Shimanaka, Trans. Iron Steel Inst. Japan., 23 (1983) 440-449.
[3] J. Iwanaga, H. Masui, J. Harase, K. Iwayama, and N. Takahasi, J. Mater. Eng. Perform., 3 (1994) 223-227.
[4] B. Zhou, C. Zhu, G. Li, X. Wan, and J. Schneider, Steel. Res. Int., 87 (2016) 1702-1714.
[5] T. Obara, H. Takeuchi, T. Takamiya, and T. Kan, J. Mater. Eng. Perform., 2 (1993) 205-210.
[6] T. Kubota, M. Fujikura, and Y. Ushigami, J. Magn. Magn. Mater., 215 (2000) 69-73.
[7] K. Iwayama and T. Haratani, J. Magn. Magn. Mater., 19 (1980) 15-17.
[8] T. Kumano, Y. Ohata, N. Fujii, Y. Ushigami, and T. Takeshita, J. Magn. Magn. Mater., 304 (2006) e602-e607.
[9] K. Hulka, C. Vlad, and A. Doniga, Steel. Res. Int., 73 (2002), 453-460.
[10] F. Fang, M.F. Lan, X. Lu, Y.X. Zhang, Y. Wang, G. Yuan, et al., J. Magn. Magn. Mater., 442 (2017) 1-7.
[11] S. Mishra and V. Kumar, Mater. Sci. Eng. B-Adv., 32 (1995) 177-184.
[12] Z.S. Xia, Y.L. Kang, X.J. Ni, Y.J. Zhou, and Q.L. Wang, J. Univ. Sci. Technol. Beijing., 31 (2009), 439. (In Chinese).
[13] N.H. van Dijk, S.E. Offerman, W.G. Bouwman, M.Th. Rekveldt, J. Sietsma, S. van der Zwaag, et al., Appl. Phys. A-Mater., 74 (2002), s978-s980.
[14] Y. Feng, J. Guo, J. Li, and J. Ning: J. Magn. Magn. Mater., 426 (2017) 89-94.
[15] M. Matsuo, T. Sakai, and Y. Suga, Metall. Mater. Trans. A., 17 (1986) 1313-1322.
[16] C. Klinkenberg, K. Hulka, and W. Bleck, Steel. Res. Int., 75 (2004) 744-752.
[17] J.S. Park, Y.S. Ha, S.J. Lee, and Y.K. Lee, Metall. Mater. Trans. A., 40 (2009) 560-568.
[18] J. Dong, F. Siciliano Jr, J. Jonas, W.J. Liu, and E. Essadiqi, ISIJ. Int., 40 (2000) 613-618.
[19] J. Schneider, G. Li, A. Franke, and B. Zhou, J. Magn. Magn. Mater., 424 (2017) 26-32.
[20] M. Hillert, Acta. Mater., 13 (1965) 227-238.
[21] F.J. Humphreys, Acta. Mater., 45 (1997) 5031-5039.
[22] Y. Shimizu, Y. Ito, and Y. Iida: Metall. Mater. Trans. A., 17 (1986) 1323-1334.
[23] S. Mishra, C. Därmann, and K. Lücke, Metall. Mater. Trans. A., 17 (1986) 1301-1312.
[24] H. Wu, L. Du, and X. Liu, J. Mater. Sci. Technol., 27 (2011) 1131-1138.
[25] S.M. Shin, S. Birosca, S.K. Chang, and B.C. De Cooman, J.Microsc-Oxford., 230 (2008) 414-423.
[26] H.T. Liu, S.J. Yao, Y. Sun, F. Gao, H.Y. Song, G.H. Liu, et al., Mater. Charact., 106 (2015) 273-282.